

Article

Discharge Coefficients of Standard Spillways at High Altitudes

Víctor Rendón ¹, Martí Sánchez-Juny ^{2,*}, Soledad Estrella ², Marcos Sanz-Ramos ², Percy Rucano ¹
and Alan Huarca Pulcha ¹

¹ Departamento de Ingeniería Civil, Universidad Nacional de San Agustín de Arequipa, Arequipa 04000, Peru; vrendon@unsa.edu.pe (V.R.); prucano@unsa.edu.pe (P.R.); ahuarcapu@unsa.edu.pe (A.H.P.)

² Flumen Research Institute, Universitat Politècnica de Catalunya-CIMNE, 08034 Barcelona, Spain; soledad.estrella@upc.edu (S.E.); marcos.sanz-ramos@upc.edu (M.S.-R.)

* Correspondence: marti.sanchez@upc.edu

Abstract: This paper presents an experimental campaign conducted next to the Condoroma dam, in Perú, at 4075 m a.s.l. The tests carried out in this paper were conducted in a 21 m long channel located at the toe of Condoroma dam. The setup consisted of a series of standard profile spillways with a vertical upstream face of up to five different dimensionless heights (P/H_d) ranging from 0.5 to 2. The experimental results indicated that, the P/H_d ratio influences the discharge coefficients in Condoroma, and $P/H_d \geq 1$ values are recommended for the design of the spillway profile. In addition, for all the P/H_d ratios studied, the discharge coefficients adjusted to the Condoroma altitude were lower than those reported by classical formulations used in conventional spillway designs. Finally, a generalized equation is proposed to estimate the discharge coefficient for standard spillways located in dams at similar elevations above sea level.

Keywords: ogee profile; discharge coefficients; atmospheric pressure; high altitude



Citation: Rendón, V.; Sánchez-Juny, M.; Estrella, S.; Sanz-Ramos, M.; Rucano, P.; Huarca Pulcha, A. Discharge Coefficients of Standard Spillways at High Altitudes. *Designs* **2024**, *8*, 22. <https://doi.org/10.3390/designs8020022>

Academic Editors: De-Cheng Feng, Ji-Gang Xu, Xuyang Cao and Luis Le Moyne

Received: 12 December 2023

Revised: 20 February 2024

Accepted: 24 February 2024

Published: 1 March 2024



Copyright: © 2024 by the authors. Licensee MDPI, Basel, Switzerland. This article is an open access article distributed under the terms and conditions of the Creative Commons Attribution (CC BY) license (<https://creativecommons.org/licenses/by/4.0/>).

1. Introduction and Objective

Generally, dams in Andean countries such as Peru are built at high altitudes, approximately 4000 m a.s.l., because most of the rainfall that occurs there. The topography of these regions allows for the storage of larger volumes of water.

The classic hydraulic design of these structures is based on previous experimental investigations carried out at lower altitudes, mainly near sea level. However, the atmospheric pressure at sea level is usually considered to be 1013 millibars, corresponding to a piezometric head (p/γ) of 10.33 m of water column, which decreases as the altitude increases. Thus, at 4075 m a.s.l., it is 621 millibars or 6.33 m of water column. It has been shown that a low atmospheric pressure decreases the performance of turbines and hydraulic pumps, as can be seen in CFD analysis by Karpenko and Bogdevičius [1]. This lower performance is mainly due to the lower oxygen concentration at this altitude. Similarly, other studies analyze the effect of air densities at high altitudes [2,3].

Since the Condoroma dam in Peru became operational, its managers have noticed that the spillway is behaving in a way that was not foreseen in the project. This malfunction was attributed to the high altitude at which the Condoroma dam is located and is the main motivation for this investigation. Therefore, the objective of this work aims to address the knowledge gap on the hydraulic behavior of discharge coefficients in standard spillways at high altitudes.

For this purpose, an experimental hood was designed to test five standard spillway profiles designed according to the United States Bureau of Reclamation criteria [4], for a wide range of approach depths P/H_d and for head conditions less than ($H < H_d$) and greater than the design head ($H_d < H$).

The standard spillway literature is reviewed and the test facilities and instrumentation used are described. The results are discussed, and the conclusions are presented.

As a summary of the current study, new formulations are developed for the discharge coefficients as a function of different approach depths. These equations present a good fit, considering the large amount of data on which they are based. They also highlight the need for further research on the hydraulic behavior of spillways under more unfavorable conditions than usual.

Previous Studies

Equation (1) is the general equation that describes the capacity of an overflow spillway [5,6].

$$Q = 2/3 ML\sqrt{2g} \left[(V_a^2/2g + h)^{3/2} - (V_a^2/2g)^{3/2} \right] \tag{1}$$

where M is the dimensionless discharge coefficient, L is the spillway length, g is the gravity acceleration, V_a is the mean approach velocity at the measurement station and h is the height above the spillway crest (Figure 1).

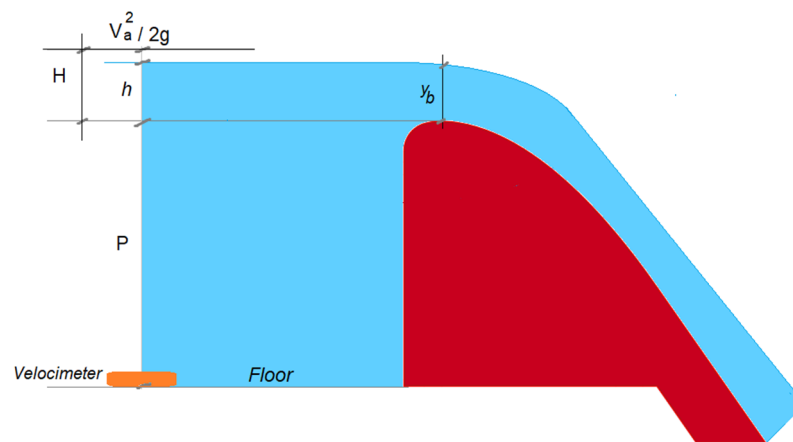


Figure 1. Sketch of a standard spillway.

Several authors group the 2/3 coefficient with the discharge coefficient M , resulting in the relationship used in the present article for the adjustment of these coefficients (m); furthermore, the velocity head $(V_a^2/2g)^{3/2}$ can be omitted from Equation (1), resulting in:

$$Q = mL\sqrt{2g}(V_a^2/2g + h)^{3/2} = mL\sqrt{2g}H^{3/2} \tag{2}$$

Equation (2) is also commonly presented by grouping the discharge coefficient (M), the integration term (2/3) and the gravity acceleration in a dimensional discharge coefficient (C).

$$Q = CLH^{3/2} \tag{3}$$

If the flow rate on a spillway is lower than the designed then $H < H_d$, positive relative pressures will occur on its bed, therefore, and the value of the discharge coefficient will tend to decrease. On the contrary, if the flow rate is higher than the designed $H > H_d$, subatmospheric pressures will occur on the spillway bed, and the discharge coefficient will increase.

Numerous researchers have studied the characteristics of standard spillway profiles. Here we present a historical synthesis, with an emphasis on contributions related to discharge coefficients. However, to the best of our knowledge, we have not found any reference to the effect that altitude can have effect on the behavior of the discharge coefficients of a spillway.

In 1907, Horton of the United States Geological Survey reported on the discharge coefficients and formulas used in spillways [7] based in experimental data obtained in Cornell University (150 m a.s.l.); however, it was Mueller, in 1908, who emphasized the importance of adapting the spillway profile on its downstream face to match the lower

nappe of a sharp-crested weir to ensure atmospheric pressure [8]. This recommendation was adopted by Morrison and Brodie in 1916 [9] and by Creager in 1917 [10].

In 1930, Nagler and Davis, based on their analysis of the Keokuk Dam (173 m a.s.l.), observed that the discharge coefficients of the model and prototype were similar and the percentage of error found was a result of the inherent inaccuracies in the experimental measurements. These inaccuracies, relative to the roughness of the crest of the model and prototype, produced differences that could be considered insignificant [11].

Dillmann, in 1933, conducted experiments for a design head of $H_d = 0.05$ m and, in reference to the discharge coefficients, showed that H_d could be exceeded by up to 300% while the flow remained stable [12,13]. In 1935, Rouse and Reid demonstrated that the flow characteristics of a spillway operating at the design head are essentially the same as those of the corresponding sharp-crested weir, showing that the discharge coefficients obtained were in agreement with those obtained by Dillman [13]. In the same year, Doland introduced a new formula for the coefficient that included a constant K and the radius of curvature of the crest [14].

Several authors proposed abacuses or potential-type equations:

$$m = m_0(H/H_d)^n \tag{4}$$

or

$$C = C_0(H/H_d)^n \tag{5}$$

which related the operation and the design heads (H/H_d) to the discharge coefficient, with m_0 or C_0 representing the corresponding value of the coefficient for the design head H_d .

Brudenell, discussing Doland's work, proposed a formula for the discharge coefficient of Equation (3) [15,16].

$$C = 3.97(H/H_d)^{0.12} \tag{6}$$

Vitols, in 1936, introduced to Bernoulli's equation the centrifugal force, which accompanies curvilinear motion and reduces the pressure between the flow and the spillway bed. The result is suction in that region and an increase in the discharge coefficient [17].

In 1937, Randolph Jr., in the Madden Dam studies (76 m a.s.l.), established a formula for the coefficient similar to Brudenell's equation [18].

$$C = 3.93(H/H_d)^{0.17} \tag{7}$$

In 1938, Borland formulated a procedure for fitting the discharge coefficients of a sharp-crested weir to a round-crest spillway (ogee) [19]. Bradley, in 1947, made improvements to the design of spillway sections at the University of Illinois Urbana [20]. In 1948, the Bureau of Reclamation (USBR) proposed a shape for standard-profile spillways [21] from the experimental study developed in their laboratory at Fort Collins-Colorado (1500 m a.s.l.).

In 1959, Webster reported that the spillway crests in Chief Joseph and The Dalles dams were designed with 75% of the maximum expected head ($0.75H_{max}$), and that if the maximum head was reached, negative relative pressures would occur on the spillway crest, increasing the discharge coefficient. This result allowed for significant cost savings in the structures by reducing the lengths of the spillways [22]. In 1964, Cassidy performed experimental tests at the University of Missouri (210 m a.s.l.) with a design load of $H_d = 0.08$ m and ratios of $P/H_d = 2.5$ and 3.3 and compared them with the results from the potential flow theory. The analytical results were 2% higher than the experimental ones [23]. In 1970, Cassidy extended his experiments to include ratios of $P/H_d = 2, 3.70$ and 6.6 , reaching $H/H_d = 3.25$, and concluded that designing spillways based on a certain percentage of H_{max} would increase the discharge coefficient, especially when considering the suction that would occur [24]. In the same year, Abecasis concluded that the value of this percentage of H_{max} should not be fixed, but that the design should be carried out according to the suction values produced on the spillway crest [25].

Also in 1970, Melsheimer and Murphy of the Waterways Experiment Station (WES) (38 m a.s.l.) analyzed various shapes of the upstream face of the spillway, designing four spillways with a head $H_d = 0.3$ m in a channel of width 0.73 m, with ratios of $P/H_d = 2.5$ and 3.4; they estimated the discharge coefficients and recorded pressures at the spillway [26]. In 1977, Senturk adjusted a value for the coefficient $m = 0.4956(H/H_d)^{0.16}$ [27].

In 1985, Maynord conducted measurements, at the Waterways Experimental Station, in a channel of width 0.762 m, with heads $H_d = 0.244$ m and $H/H_d = 0.4$ to 1.5, and values of $P/H_d = 0.25, 0.50, 1.00$ and 2.00, to adjust his discharge coefficients [28].

In 1991 at the Federal Institute of Technology in Zurich (495 m a.s.l.), Hager obtained the discharge coefficients for different operating heads from two spillways of different geometries, with a face height $P = 0.70$ m, in a channel of width of 0.50 m, and with different design heads [29].

Sanieie et al., in 2016 [30], studied the scale effects on the discharge coefficients of ogee spillways with an arc in plan and converging training walls. Their results revealed that, by using the Froude similarity, the effect of viscosity and surface tension increases resulted in a lower discharge coefficient. They showed that, for values

$$We^{0.6} Re^{0.2} > 350 \quad (8)$$

with We being the Weber number and Re the Reynolds number, it is possible to neglect the effect of viscosity and surface tension.

In 2018, Erpicum et al. [31] investigated four high-head standard spillways in the hydraulic laboratory of the University of Liege (240 m a.s.l.). They evaluated the discharge coefficients of these spillways up to head ratios of five and reported that the discharge coefficient increases monotonically with the head. Three of the spillways fulfilled the following potential function:

$$m = 0.501(H/H_d)^{0.12} \quad (9)$$

Also in 2018, Alwan and Al-Mohammed [32] estimated a power function between the discharge coefficient and the upstream water depth of a rectangular notch using a dimensional analysis technique.

In 2019, Aguilera and Jimenez [33] applied a 3D numerical model for flow simulation in spillways. Their results show that the discharge coefficients present a difference of less than 1% with respect to those recommended by USBR, for P/H ratios higher than 1.0. For lower values, the software calculates a higher discharge capacity, which increases as the P/H ratio decreases. The effect of converging walls was also investigated in 2019 [34], and resulted in lower values of the discharge coefficient values than those of the Bureau of Reclamation spillway due to flow convergence itself.

Hoseini et al., in 2020 [35], applied the convex streamline theory to formulate the discharge coefficient and crest section velocity profile of a quarter-circle crested spillway at design head, and compared these results with experimental data from 11 models of a quarter-circle crested weir.

Alkhamis et al., in 2021 [36], also used CFD numerical evaluation to predict the discharge coefficients over an ogee-shaped crest. In the same year, Haktanir and Khalaf [37] analyzed the discharge coefficients for radial-gated ogee spillways and concluded that the results in [4] are not sufficient to accurately estimate the discharge over an ogee spillway for the case of partially open gates.

In 2022, Salmasi and Abraham [38] analyzed the influence of the upstream slope of the spillway and the downstream submergence. Their results showed that, for all standard ogee spillways, the discharge coefficient (C) increases with increasing P/H , and then reaches a constant value. Regarding the value of the discharge coefficient, it decreases from 2.25 under free-flow conditions to 2.15 under submerged flow conditions.

In the same year, Stilmant et al. [39] studied the derivation of a theoretical model that relates H/H_d , independently of empirical coefficients, and whose predictions have a wide range of heights. They used potential flow theory, integrated in a curvilinear frame of

reference, and critical flow theory. The results show a good fit with the experimental data for ratios H/H_d between 0 and 5.

Moreover, various studies have been carried out in the last five years regarding the analysis of discharge coefficients over particular spillway types. For example: implementing antivortices to increase the discharge coefficient in lateral triangular labyrinth weirs by [40], the effects of geometric parameters in trapezoidal–triangular labyrinth weirs [41], the behavior in horizontal crested weirs under free-flow conditions [42], the variation with respect to discharge coefficients in round-crested weirs [43], the impact of the upstream orientation angle on the discharge coefficient in wide-crested trapezoidal weirs [44], the appropriate use of modeling approaches for the determination of discharge coefficients in lateral rectangular weirs [45,46], and predictive models [47]. Nevertheless, neither past nor recent empirical investigations have been conducted at high altitudes, such as at Condoroma.

Table 1 presents the main characteristics of the tests carried out in classical studies of the discharge coefficient in ogee spillways and the altitude where the experiments were conducted. The table also includes the parameters studied in the present investigation at 4075 m a.s.l.

Table 1. Main characteristics of the tests documented in the present work.

Author	Width (m)	H_d (m)	P/H_d	Q (L/s)	Elevation m a.s.l.
Dillman [12]	-	0.05	-	-	520
Cassidy [24]	-	-	2; 2.5; 3.7; 6.6	-	210
Rouse [48]	0.500	-	-	62	115
Murphy [26]	0.732	0.305	3.5; 7.0	560	38
Maynard [28]	0.762	0.249	0.25; 0.5; 1.0; 2.0	385	38
Hager [29]	0.500	0.20/0.1	3.5/7.0	375	495
Epicum [31]	0.200	0.10/0.15	-	358	240
Condoroma dam	0.915	0.20/0.175	0.25; 0.5; 1; 1.5/2	415	4075

2. Materials and Methods

2.1. Experimental Facility

The tests carried out in this paper were conducted in a 21 m long channel located at the toe of Condoroma dam (Figure 2) in southern Peru, in the Department of Arequipa, at an altitude of 4075 m a.s.l. The channel is divided into three sections (Figure 3b): the water intake zone is 1.83 m wide, 9.00 m long and 1.10 m high; the test zone is 0.915 m wide, 8.10 m long and 0.75 m high; and finally, the outlet reach presents a difference in level of 0.70 m over a length of 3.90 m. It is 0.915 m wide and 0.75 m high.



Figure 2. General view of the 21 m long experimental channel located close to Condoroma dam at 4075 m a.s.l.

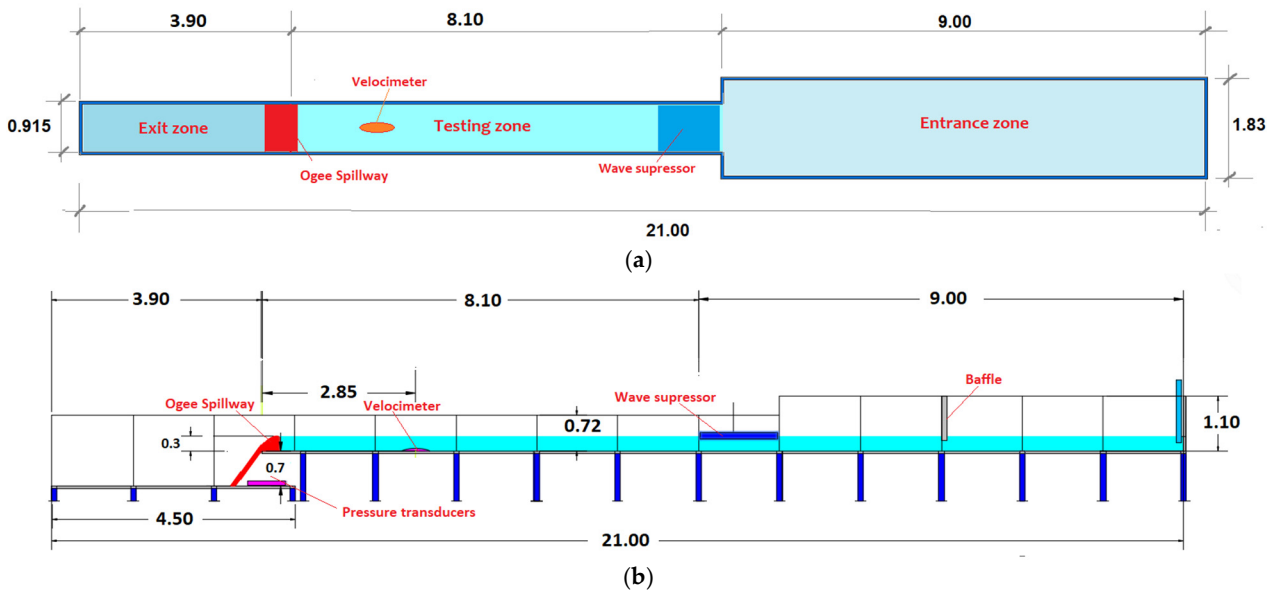


Figure 3. (a) Plan view and (b) profile of the hydrodynamic channel.

Five ogee spillways were tested, each designed according to USBR criteria [4], with different upstream face heights P . The assumed design head is $H_d = 0.20$ m for faces $P = 0.30$ m, 0.20 m, 0.10 m and 0.05 m, and $H_d = 0.175$ m for the face $P = 0.35$ m. These values correspond to $P/H_d = 2, 1.50, 1, 0.5$ and 0.25 . In addition, there is a vertical drop of 0.70 m. Figure 4a shows the spillway for $P/H_d = 2$ and Figure 4b shows the spillway for $P/H_d = 0.5$.



Figure 4. View of two of the ogee-tested profiles: (a) $P/H_d = 2$; (b) $P/H_d = 0.5$. Additionally, $P/H_d = 1.5, 1$ and 0.25 were tested.

2.2. Instrumentation

The experimental model was equipped with a Sontek-IQ Plus current meter (Figure 5a), which measures velocity in the range of 0 to 5 m/s with an accuracy of ± 0.005 m/s, depth with an accuracy of ± 0.003 m, pressure sensor accuracy 0.1% of full scale, and temperature $\pm 0.2\%$ of full scale. The velocity measurement was based on a 3 MHz Doppler Acoustic Profiler.



Figure 5. (a) Sontek current meter—IQ plus; (b) pumping system.

The flume was fed by a pumping system (Figure 5b) that draws water from the head chamber of the Condoroma dam hydroelectric power plant and can supply up to 415 L/s.

2.3. Operating Conditions

The different spillways were set up according to their different face heights (P), as mentioned above, and operated at flow rates between 53 L/s and 363 L/s. Each test was performed by measuring the flow rate and water depth every 10 s for at least 5 min. The stability of the free surface in the approaching flow made it possible to guarantee the quality of this acquisition frequency, as will be shown in the next section.

With respect to the location of the measurement zone, it can be specified that the whole cross section participates uniformly in the discharge. No significant vertical accelerations were observed, so it can be accepted that the pressure distribution follows, approximately, hydrostatic behavior.

It is known that, in a flow with a free fall, the measuring section should be located between 3 and 4 times the critical head upstream of the fall [49]. Rouse [50], in sharp-crested weirs with 62.5 L/s, reported that the curvature of the nappe reached up to 0.90 m upstream of the spillway crest. Therefore, it is considered appropriate, in the present experimental campaign, to measure between 2.68 and 2.75 m from the spillway crest, even for the higher flow rate tested.

For each case, it was ensured that the head in the measurement zone (Figure 1) exceeded $h = 0.10$ m to ensure that the head at the spillway crest (y_b) always remained above 0.05 m ($y_b > 0.05$ m). This prevented the scale effects produced by viscosity and surface tension, as recommended by Schoder and Turner ($y_b > 0.06$ m) [51], Eisner ($y_b > 0.049$ m) [52], Ghetti ($y_b > 0.05$ m) [53] and Vischer and Hager ($y_b > 0.10$ m) [54], with Hager et al. subsequently indicating values of at least $y_b > 0.05$ m [55] and Carrillo et al. of $h > 0.045$ m [56]. Also, taking into account the depths and velocities at the crest for each spillway analyzed with different P/H_d , which are described in Section 3, it can be concluded that in any case the Equation (8) produces values greater than 350, which, according to Saneie et al. [30], allows us to ignore the effects of viscosity and surface tension.

2.4. Methodology

The long duration of the tests, around 5 min each, generated a large amount of experimental data which, as shown in Section 3.1, showed a certain dispersion (Figure 6). It was proposed to process the data in order to verify that this variability was within the expected error ranges of the measuring devices, as well as to detect the possible existence of outliers.

To analyze the variability of the data series, a dispersion analysis was carried out and represented graphically by means of boxplots (Figure 7). On the other hand, the

detection of outliers was carried out using the classical technique of interquartile range (IQR method) [57–59]. Finally, once processed, the time series of each test were summarized to their mean value for its final analysis.

3. Results

Equation (1) was used for the different flow rates tested. Likewise, the discharge coefficient m , was determined from Equation (4). The following subsections present the adjusted coefficients for the different spillway heights P and the different rates H/H_d .

3.1. Data Processing

The water level and flow rate data recorded during the tests in the case of $P/H_d = 2$ are shown in Figure 6a, while Figure 6b shows the direct estimation of the drainage coefficients resulting from the former. The resulting scatter can be seen in both graphs. For each group of tests, a variability analysis of the values recorded during the tests was carried out using boxplots.

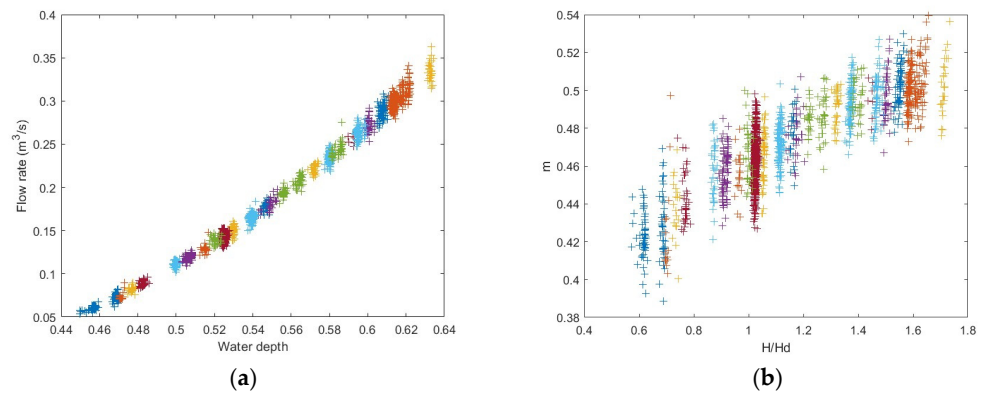


Figure 6. (a) Water depth (in m) and flow rates measured for the case $P/H_d = 2$, test duration > 5 min; (b) relation between discharge coefficients and the dimensionless head H/H_d obtained from the measured data in (a).

From the boxplot analysis, it can be seen that the water depth data (Figure 7a) showed little variability and oscillated within the measurement error interval of ± 0.003 m. On the other hand, the flow rate values (Figure 7b) showed greater variability due to the inherent noise in the Doppler Acoustic Profiler measurements and the fact that the water used could have different concentrations of impurities depending on the day, which could result in more or less noise in the velocity sensor readings. For this reason, the interquartile range (IQR) method [57] was used to detect outliers in the recorded flow rate data.

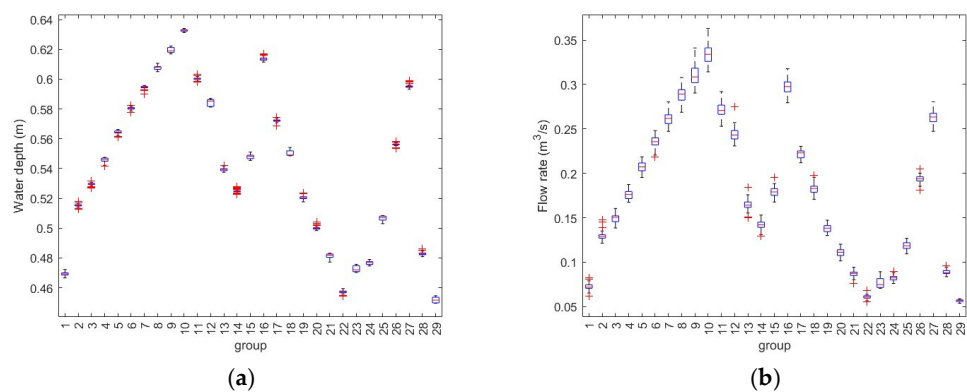


Figure 7. Boxplot graphs for the tests on $P/H_d = 2$ related to (a) water depth and (b) flow rate measurements.

Figure 8a shows the recorded values of water depth and Figure 8b flow rate after removing the outliers. The thick black dots represent the average value obtained for each test. These averages will be used in the data analysis from now on.

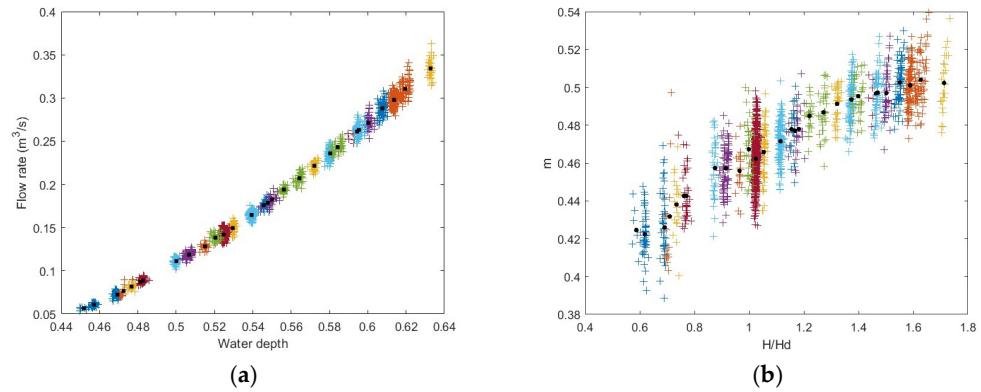


Figure 8. (a) Water depth (in m) and flow rates after the detection of outliers; (b) relation between discharge coefficients (m) and the dimensionless head (H/H_d) after the detection of outliers. The thick black dots correspond to the average values.

3.2. Spillway $P/H_d = 2.0; 1.5; 1; 0.5; 0.25$

Table 2 shows a summary of the main characteristics of the Condorama tests. Taking as a reference the potential function described in Equation (4), for the discharge coefficient used by Brudenell [15], Randolph [18], Senturk [27] and Erpicum [31], the processed data ($m, H/H_d$) were transformed into a logarithmic form [58,59]. The graph of the residuals and the fitted regression curve, for the parameters $P/H_d = 2, 1.5, 1.0, 0.5$ and 0.25 , indicated a good fit. Figure 9a,b show the graphs obtained for the tests with $P/H_d = 2$.

Table 2. Main characteristics of the tests in Condorama.

P (m)	P/H_d	Q (L/s)	Stage (m)	Fr	y_b (m)	Fr_b
(1)	(2)	(3)	(4)	(5)	(6)	(7)
0.35	2.0	53–363	0.45–0.634	0.062–0.25	0.073–0.21	0.96–1.28
0.30	1.5	49–400	0.40–0.607	0.068–0.31	0.074–0.24	0.85–1.18
0.20	1.0	52–415	0.30–0.492	0.11–0.42	0.074–0.23	0.89–1.29
0.10	0.50	56–391	0.20–0.368	0.22–0.62	0.086–0.21	0.78–1.40
0.05	0.25	61–345	0.15–0.280	0.37–0.93	0.100–0.22	0.63–1.15

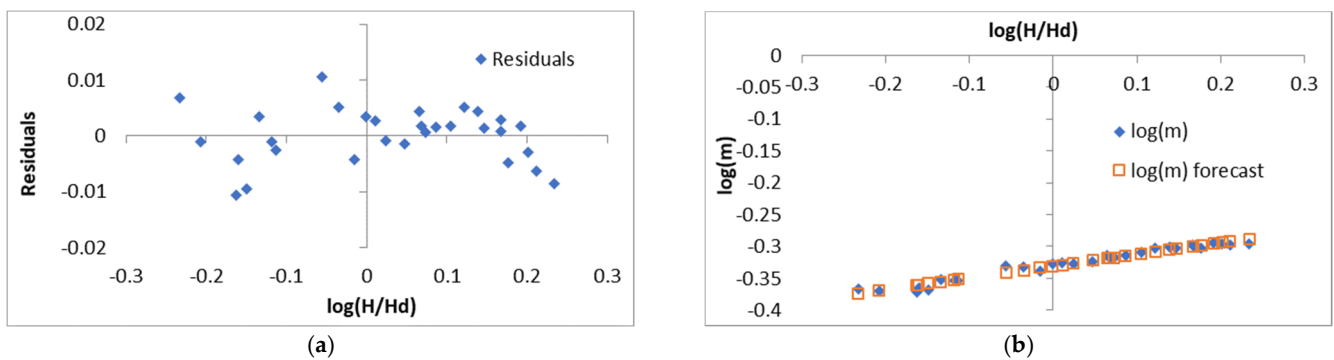


Figure 9. $P/H_d = 2$. (a) Graph of residuals of the fitted regression; (b) fitted regression curve.

The coefficients found in the regression analysis were then calculated, which allowed us to determine m_0 , the exponent n and the coefficient of determination R^2 . Table 3 summarizes, for each value of P/H_d , the values of m_0 , n and R^2 , obtained from the experimental campaign conducted at Condorama. The table also compares the results with data from other studies that used the same or a similar relationship between the height (P) and the design head (H_d).

Table 3. P/H_d ratio and discharge coefficient m adjustment factors of Equation (4).

P/H_d	Data	m_0	n	R^2
2.0	Condorama	0.467	0.184	0.962
2.0	Maynard [28]	0.494	0.157	0.984
2.0	Cassidy [24]	0.518	0.186	0.993
2.5	Murphy [26]	0.503	0.139	0.974
3.5	Hager [29]	0.493	0.122	0.988
1.5	Condorama	0.470	0.172	0.969
1	Condorama	0.472	0.158	0.974
1	Maynard [28]	0.490	0.129	0.989
0.5	Condorama	0.480	0.098	0.82
0.5	Maynard [28]	0.487	0.099	0.849
0.25	Condorama	0.465	0.085	0.807
0.25	Maynard [28]	0.468	0.063	0.489

Figure 10 compares the Condorama data with those obtained by Maynard et al. [28] for $P/H_d = 2.5$ and Hager [29] for $P/H_d = 3.5$ and Figure 11 shows the discharge coefficients for the tests $P/H_d = 1.5, 1, 0.5$ and 0.25 .

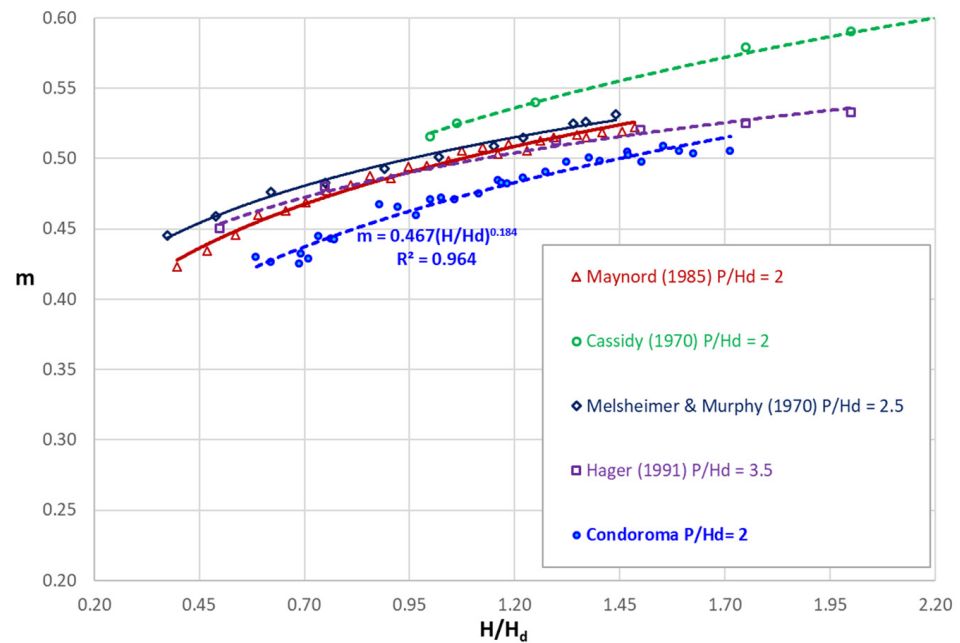


Figure 10. Adjustment of the dimensionless discharge coefficient for the case $P/H_d = 2.0$ and comparison with the results of Maynard et al. [28], Cassidy [24], Melsheimer and Murphy [26] and Hager [29].

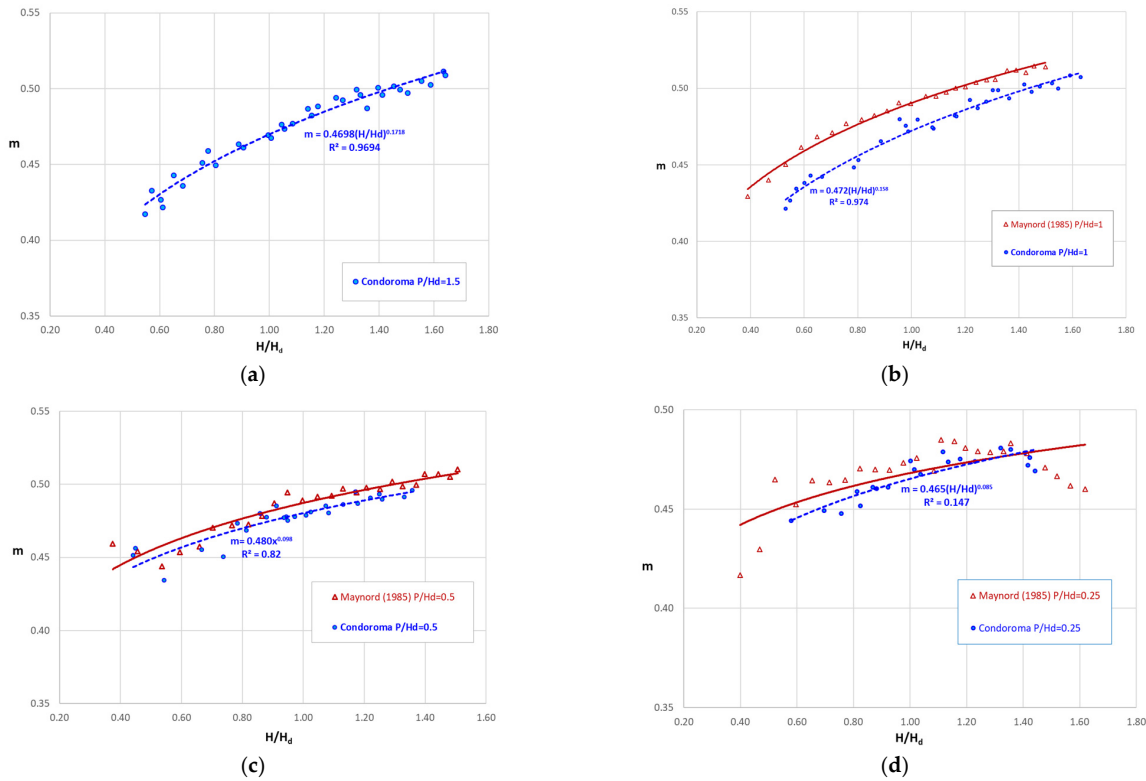


Figure 11. (a) $P/H_d = 1.5$; (b) $P/H_d = 1.0$; (c) $P/H_d = 0.5$; (d) $P/H_d = 0.25$. Adjustment of the dimensionless discharge coefficient for the case $P/H_d = 1; 0.5; 0.25$ and comparison with the results obtained by Maynard [28].

3.3. P/H_d Aggregated Analysis

In Figure 12, the Condoroma experimental data are plotted for all ratios P/H_d , showing the relationship between the operating and design heads H/H_d on the horizontal axis and the discharge coefficient m on the vertical axis. The data are compared in Figure 12a with the values fitted from the equations proposed by Brudenell [15], Randolph [18], Senturk [27] and Erpicum [31]. Similarly, in Figure 12b, the data are compared with the results from Hager [29], Dillman [12], Rouse and Reid [13] and Montes [60].

Table 4 condenses the adjustment coefficients (m_o and n) of the discharge coefficient (m) of Equation (4) obtained in the different studies analyzed.

Table 4. Fitting factors corresponding to Equation (4) for the discharge coefficient m proposed by different authors.

Author	m_o	n
Dillman [12]	0.512	0.147
Rouse [13]	0.510	0.147
Brudenell [15]	0.495	0.120
Randolph [18]	0.490	0.170
Cassidy [24]	0.518	0.186
Murphy [26]	0.502	0.139
Senturk [27]	0.496	0.160
Maynard [28]	0.491	0.128
Hager [29]	0.495	0.129
Erpicum [31]	0.501	0.120
Montes [60]	0.496	0.113
Condoroma	0.470	0.151

As previously indicated, often in the works referenced in this paper, the discharge coefficients were fitted from the dimensional coefficient C of Equation (5). Figure 13, shows the comparison of the values of the dimensional discharge coefficient C obtained

from the Condoroma experimental data with those obtained by USBR [4], Maynard [28], Murphy [26] and Cassidy [24].

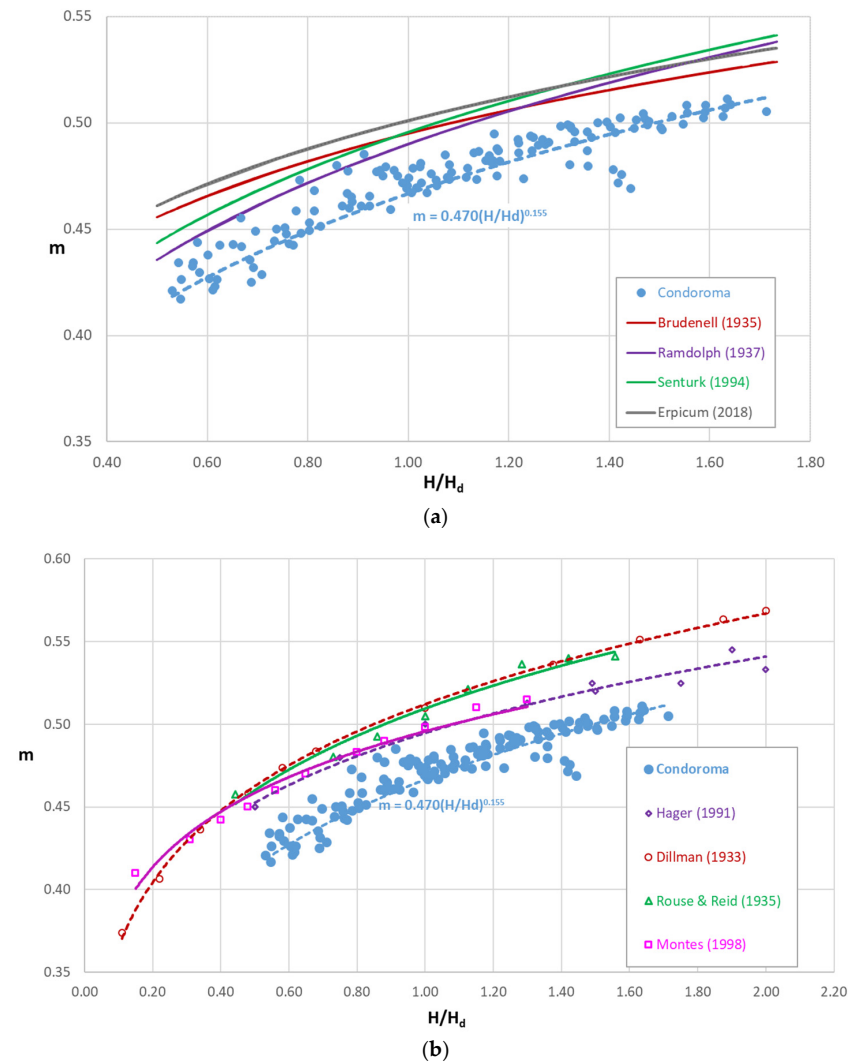


Figure 12. (a) Comparison of the values of the dimensionless discharge coefficient obtained from experimental results at Condoroma with those obtained by Brudenell [15], Randolph [18], Senturk [27] and Erpicum [31]; (b) Generalized equations for the dimensionless discharge coefficient obtained by Hager [29], Dillman [12], Rouse and Reid [13] and Montes [60].

Table 5 summarizes the coefficients (C_o and n) of the discharge coefficient (C) of Equation (5).

Table 5. Fitting factors corresponding to Equation (5) for the discharge coefficient C .

Author	C_o	n
Brudenell [15]	2.190	0.120
Randolph [18]	2.168	0.170
Cassidy [24]	2.294	0.186
USBR [4]	2.211	0.132
Murphy [26]	2.224	0.139
Maynard [28]	2.172	0.128
Condoroma	2.077	0.151

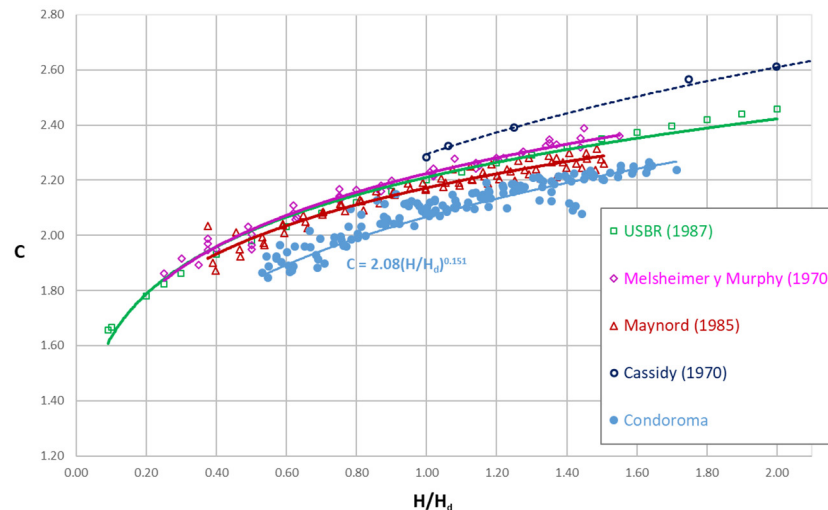


Figure 13. Comparison of the generalized equations for the dimensionless discharge coefficient obtained by USBR [4], T. Murphy [26], Maynard [28] and Cassidy [24] with the results from Condoroma.

4. Discussion

The velocity distribution in the inlet channel has a greater effect on the spillway as the channel narrows due to the disturbances introduced by the sidewalls. Considering that the width of the Condoroma channel is 0.915 m, its velocity distribution is more homogeneous compared to the other channels shown in Table 1.

The Froude number in the measurement area was subcritical for all the spillway heights analyzed, while at the spillway crest, values were obtained for both subcritical and supercritical flow (Table 2).

The scatter of the data at Condoroma is greater for lower H/H_d ratios, regardless of the approach heights P/H_d . This is because, in that case, subcritical flow, observed at the spillway crest, generates disturbances that propagate upstream, affecting the measurement area.

It has been observed that the dimensionless height ratio P/H_d has a significant influence on the discharge coefficients, adjusted for Condoroma. Experimentally, it has been found that, for heights $P/H_d \geq 1$, the flow streamlines have a greater regularity and stability, with more predictable behavior, as can be seen from the high correlation coefficients obtained from the processed data in the cases $P/H_d = 2, 1.5$ and 1 in Figures 10 and 11a,b. On the other hand, at dimensionless heights $P/H_d < 1$, a somewhat more unstable flow behavior is observed, with the appearance of waves that are difficult to attenuate, which makes it difficult to measure the water depths and ultimately introduces uncertainty in the adjustment of the respective discharge coefficients (Figure 11c,d).

From the analysis of Figures 10 and 11, it can be also seen that the discharge coefficient increases directly proportional to the ratio H/H_d . Furthermore, the discharge coefficient is influenced by the height of the facing P : when the ratio $P/H_d \geq 1$ and $H/H_d > 1$, the discharge coefficients are higher than those with $P/H_d < 1$, and lower the lower the facing height. Besides, although the tests with $P/H_d \geq 1$ at Condoroma show significantly lower values than those obtained in previous experiences at much lower altitudes, it can be seen that the tests for $P/H_d < 1$ the discharge coefficients, although still significantly lower, are more similar to the results obtained by other authors.

The m_o values (see Table 3) of the discharge coefficient for the dimensionless design head (Equation (4)) obtained from the Condoroma data, are consistently lower than those reported by Maynard [28], with a maximum difference of 5.78% for $P/H_d = 2$ and a minimum difference of 1.5% for $P/H_d = 0.50$. In Cassidy [24], for $P/H_d = 2.0$, the difference is 10.9%. Regarding the exponent n , the values at Condoroma, compared with those of Maynard [28], are higher for $P/H_d = 2, 1$ and 0.25 , varying between 15% and 67%; and lower by 1% for $P/H_d = 0.5$.

Table 3 shows that the m_o values presented by the different authors analyzed vary between 0.49 [18] and 0.518 [24], while the Condorama results show a value of 0.470.

When analyzing all the m_o values (Table 4) obtained for the P/H_d ratios tested at Condorama, it is evident that they are lower by 4% and 10% than the values presented by Randolph Jr. [18] and Cassidy [24], respectively. Regarding the coefficients of determination R^2 , for $P/H_d = 2, 1.5$ and 1 , the lowest value is 0.962, which is high enough considering the number of data points on which it is based.

Regarding $P/H_d = 0.5$, the R^2 is 0.82, a value lower than that reported by Maynard ($R^2 = 0.85$) [28]. For $P/H_d = 0.25$, the R^2 is 0.807, higher than that calculated for the Maynard data of 0.49 [28]. Both ratios $P/H_d = 0.5$ and 0.25 are not recommended for design because, as reported by Maynard [28], they exhibit many instabilities.

Figure 14 shows the coefficient C_o of Equation (5) when the ogee is formed to the ideal nappe shape; that is, when $H/H_d \approx 1$ for the five spillways heights tested at Condorama, in addition to the curve proposed by USBR [4]. When the weir height $P = 0$, the vertical contraction is suppressed and it becomes a control section, for which the theoretical $C_o = 1.70$ [4]. Also, while the USBR suggests that, for the case $H/H_d = 1$, from the values of P/H_d , C_o tends towards 2.17, the Condorama data seem to tend towards a slightly lower value of 2.1.

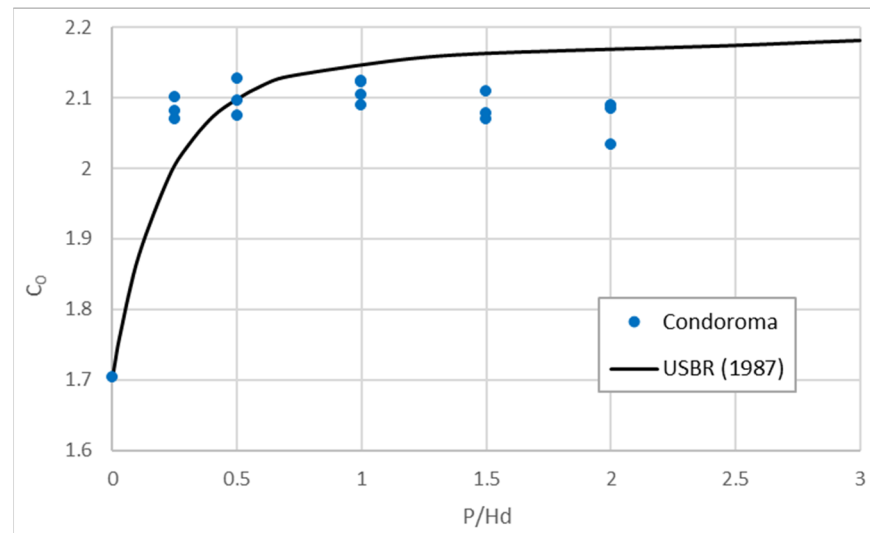


Figure 14. C_o coefficient of Equation (5) for the Condorama design head compared with that proposed by USBR [4].

In view of the experimental results reported in the present paper on a family of spillways of dimensionless height P/H_d of values 2, 1.5, 1, 1, 0.5 and 0.25 at heights of approximately 4000 m a.s.l., for values of H/H_d ranging between 0.54 and 1.65, it is suggested to adjust the discharge coefficient via the following equations:

$$m = 0.470 \left(\frac{H}{H_d} \right)^{0.151} \tag{10}$$

$$C = 2.077 \left(\frac{H}{H_d} \right)^{0.151} \tag{11}$$

5. Conclusions

This work explores the influence of atmospheric conditions in high-altitude areas on the discharge coefficients of ogee spillways. To achieve this objective, an experimental campaign was carried out at an altitude of 4075 m a.s.l., and the recorded data have been compared with those obtained previously. The main conclusions drawn are the following:

- The experimental results were compared with previous research. At altitudes above 4000 m a.s.l., the discharge coefficients show substantial differences, with consistently lower values than those obtained to date in previous works conducted at lower altitudes above sea level.
- Particularly, the discharge coefficient C_o of Equation (5) when $H/H_d \approx 1$ at Condoroma seems to tend towards a value slightly lower than 2.1, lower than the 2.17 proposed by USBR [4].
- The P/H_d ratio influences the discharge coefficients in Condoroma, and $P/H_d \geq 1$ values are recommended for the design of the spillway profile. The authors observed more stable and predictable flow behavior for higher P/H_d ratios.
- Although the results obtained for $P/H_d \geq 1$ at Condoroma show significantly lower values than those obtained in previous experience at much lower altitudes, it can be seen that the tests for $P/H_d < 1$ the discharge coefficients, although still significantly lower, are more similar to the results obtained by other authors.
- The equations to determine the discharge coefficients (Equations (10) and (11)) for Condoroma could be used in areas at similar altitudes in the absence of experimental data.

Author Contributions: Conceptualization, V.R. and M.S.-J.; methodology, V.R. and M.S.-J.; software, V.R., M.S.-J., S.E. and M.S.-R.; validation, V.R., M.S.-J., S.E., M.S.-R. and A.H.P.; formal analysis, V.R., M.S.-J., S.E., M.S.-R., P.R. and A.H.P. and; investigation, V.R., M.S.-J., S.E., M.S.-R., P.R. and A.H.P.; resources, V.R., M.S.-J., S.E., M.S.-R., P.R. and A.H.P. data curation, V.R. and M.S.-J.; writing—original draft preparation, V.R., M.S.-J., S.E., M.S.-R., P.R. and A.H.P.; writing—review and editing, V.R., M.S.-J., S.E., M.S.-R., P.R. and A.H.P.; visualization, V.R., M.S.-J., S.E., M.S.-R., P.R. and A.H.P.; supervision, V.R. and M.S.-J.; project administration, V.R. and M.S.-J.; funding acquisition, V.R. All authors have read and agreed to the published version of the manuscript.

Funding: This research was financed by the Universidad Nacional de San Agustín de Arequipa—Peru, through financing contract No. 0042-2016-UNSA.

Data Availability Statement: Some or all data, models, or codes that support the findings of this study are available from the corresponding author upon reasonable request.

Acknowledgments: We would like to thank Universidad Nacional de San Agustín de Arequipa, UNSA, Arequipa, Perú. This article was supported by a Research Project under the contract IBA-IB-0042-2016-UNSA.

Conflicts of Interest: The authors declare no conflicts of interest.

References

1. Karpenko, M.; Bogdevičius, M. Investigation of Hydrodynamic Processes in the System—“Pipeline-Fittings”. In *TRANSBALTICA XI: Transportation Science and Technology: Proceedings of the International Conference TRANSBALTICA, Vilnius, Lithuania, 2–3 May 2019*; Springer International Publishing: New York, NY, USA, 2020; pp. 331–340. [[CrossRef](#)]
2. Han, Q.; Qu, J.; Dong, Z.; Zhang, K.; Zu, R. Air density effects on aeolian sand movement: Implications for sediment transport and sand control in regions with extreme altitudes or temperatures. *J. Sedimentol.* **2015**, *62*, 1024–1038. [[CrossRef](#)]
3. Van Ingen Schenau, G.J. The influence of air friction in speed skating. *J. Biomech.* **1982**, *15*, 449–458. [[CrossRef](#)]
4. United States Bureau of Reclamation. *Design of Small Dams*, 1960th, 1973th, 1977th ed.; Bureau of Reclamation: Denver, CO, USA, 1987.
5. Naudascher, E. *Hidraulica de Canales*; Limusa: Mexico City, Mexico, 2002.
6. Russell, G. *Hydraulics*, 5th ed.; Henry Holt and Company: New York, NY, USA, 1948.
7. Horton, R.E. *Weir Experiments, Coefficients, and Formulas*; Water Supply and Irrigation Paper N°. 200; U.S. Geological Survey: Reston, VA, USA, 1907.
8. Mueller, R. Development of Practical Type of Concrete Spillway Dam. *Eng. Rec.* **1908**, *58*, 461.
9. Morrison, E.; Brodie, O. *Masonry Dam Design*; John Wiley & Sons, Inc.: Hoboken, NJ, USA, 1916.
10. Creager, W. *Engineering for Masonry Dams*; John Wiley and Sons: New York, NY, USA, 1917; pp. 105–110.
11. Nagler, F.; Davis, A. Experiments on discharge over spillway and models, Keokuk Dam. *Trans. Am. Soc. Civ. Eng.* **1930**, *94*, 777–820. [[CrossRef](#)]
12. Dillmann, O. *Untersuchungen an Ueberfallen*; Mitteilungen des Hydraulics Institus der T.H.: Munchen, Germany, 1933; p. 7.
13. Rouse, H.; Reid, L. Model research on spillway crest. *Civ. Eng.* **1935**, *5*, 10.

14. Doland, J. Flow over rounded crests. *Eng. News Rec.* **1935**, *114*, 551.
15. Brudenell, R. Discussion of Flow over rounded crests. *Eng. News Rec.* **1935**, *115*, 95.
16. Chow, V. *Open-Channel Hydraulics*; McGraw-Hill Book Company: New York, NY, USA, 1959.
17. Vitols, A. Vacuumless dam profiles. *Wasserkr. Wasserwirtsch.* **1936**, *31*, 207.
18. Randolph, R.J. Hydraulic tests on the spillway of the Madden Dam. *Trans. Am. Soc. Civ. Eng.* **1937**, *103*, 1080–1112. [[CrossRef](#)]
19. Borland, W. *Flow over Crest Weirs*; Civil Engineering: Fort Collins, CO, USA, 1938.
20. Bradley, J. *Refinements in the Design of Overfall Spillway Sections*; Bureau Reclamation United States: Denver, CO, USA, 1947.
21. United States Bureau of Reclamation. *Studies of Crests for Overflow Dams—Bulletin 3*; Bureau of Reclamation: Denver, CO, USA, 1948; pp. 1–5.
22. Webster, M. Spillway Design for Pacific Northwest Projects. *J. Hydraul. Div.* **1959**, *85*, 63–85. [[CrossRef](#)]
23. Cassidy, J. *Spillway Discharge at other than Design Head*; State Univesity of Iowa: Iowa City, IA, USA, 1964.
24. Cassidy, J. Designing spillway crests for high head operation. *J. Hydraul. ASCE* **1970**, *HY3*, 745–753. [[CrossRef](#)]
25. Abecasis, F. Discussion of Designing spillway crests for high head operation. *J. Hydraul. Div. ASCE* **1970**, *96*, 2654–2658. [[CrossRef](#)]
26. Melsheimer, E.; Murphy, T. *Investigations of Various Shapes of the Upstream Quadrant of the Crest of a High Spillway*; Hidraulic Laboratory Investigation: Vicksburg, MS, USA, 1970.
27. Senturk, F. *Hydraulics of Dams and Reservoirs*; Water Resouces Publications: Littleton, CO, USA, 1994.
28. Maynord, S. *General Spilway Investigation*; U. S. Army Corps of Engineers, Waterways Experiment Station: Vicksburg, MS, USA, 1985.
29. Hager, W. Experiments on standard spillway flow. *Proc. Inst. Civ. Eng.* **1991**, *91*, 399–416.
30. Saneie, M.; SheikhKazemi, J.; Azhdary Moghaddam, M. Scale Effects on the Discharge Coefficient of Ogee Spillway with an Arc in Plan and Converging Training Walls. *Civ. Eng. Infrastruct. J.* **2016**, *49*, 361–374. [[CrossRef](#)]
31. Erpicum, S.; Blancher, B.; Vermeulen, J.; Peltier, Y.; Archambeau, P. Experimental study of ogee crested weir operation above the design head and influence of the upstream quadrant geometry. In Proceedings of the 7th International Symposium on Hydraulic Structures, Aachen, Germany, 15–18 May 2018.
32. Alwan, H.H.; Al-Mohammed, F.M. Discharge coefficient for rectangular notch using a dimensional analysis technique. *IOP Conf. Ser. Mater. Sci. Eng.* **2018**, *433*, 012015. [[CrossRef](#)]
33. Aguilera, E.; Jimenez, O. Applicability of a 3D numerical model for flow simulation of spillways. In Proceedings of the 38th IAHR World Congress, Panama City, Panama, 1–6 September 2019; p. 11.
34. Roushangar, K.; Khowr, A.F.; Saniei, M. Investigating impact of converging training walls of the ogee spillways on hydraulic performance. *Paddy Water Environ. J.* **2020**, *18*, 355–366. [[CrossRef](#)]
35. Hoseini, A.; Mohammadzadeh-Habili, J. Investigation of Quarter-Circular Crested Spillway Using Experiments and Convex Streamline Theory. *Iran. J. Sci. Technol. Trans. Civ. Eng.* **2022**, *46*, 1491–1501. [[CrossRef](#)]
36. Alkhamis, M.T.; Sabbagh-Yazdi, S.-R.; Ranjbar-Malekshah, M. Numerical evaluation of discharge coefficient and energy dissipation of flow over a stepped morning glory spillway. *J. Eng. Res.* **2021**, *9*, 60–80. [[CrossRef](#)]
37. Haktanir, T.; Khalaf, M. Discharge Coefficients for Radial-Gated Ogee Spillways by Laboratory Data and by Design of Small Dams. *Tek. Dergi J. Sect.* **2021**, *32*, 1099–10945. [[CrossRef](#)]
38. Salmasi, F.; Abraham, J. Discharge coefficients for ogee spillways. *Water Supply* **2022**, *22*, 17. [[CrossRef](#)]
39. Stilmant, F.; Erpicum, S.; Peltier, Y.; Archambeau, P.; Dewals, B.; Piroton, M. Flow at an Ogee Crest Axis for a Wide Range of Head Ratios: Theoretical Model. *Water* **2022**, *14*, 2337. [[CrossRef](#)]
40. Abbasi, S.; Fatemi, S.; Ghaderi, A.; Di Francesco, S. The Effect of Geometric Parameters of the Antivortex on a Triangular Labyrinth Side Weir. *Water* **2021**, *13*, 14. [[CrossRef](#)]
41. Ghaderi, A.; Daneshfaraz, R.; Dasineh, M.; Di Francesco, S. Energy Dissipation and Hydraulics of Flow over Trapezoidal–Triangular Labyrinth Weirs. *Water* **2020**, *12*, 1992. [[CrossRef](#)]
42. Zerihun, Y.T. Free Flow and Discharge Characteristics of Trapezoidal-Shaped Weirs. *Fluids* **2020**, *5*, 238. [[CrossRef](#)]
43. Gong, J.; Deng, J.; Wei, W. Discharge Coefficient of a Round-Crested Weir. *Water* **2019**, *11*, 1206. [[CrossRef](#)]
44. Jiang, L.; Diao, M.; Sun, H.; Ren, Y. Numerical Modeling of Flow Over a Rectangular Broad-Crested Weir with a Sloped Upstream Face. *Water* **2018**, *10*, 1663. [[CrossRef](#)]
45. Di Bacco, M.; Scorzini, A.R. Are We Correctly Using Discharge Coefficients for Side Weirs? Insights from a Numerical Investigation. *Water* **2019**, *11*, 2585. [[CrossRef](#)]
46. Yarar, A.A. Analytical and artificial neural network models to estimate the discharge coefficient for ogee spillway. *E3S Web Conf.* **2017**, *19*, 03028. [[CrossRef](#)]
47. Granata, F.; Di Nunno, F.; Gargano, R.; de Marinis, G. Equivalent Discharge Coefficient of Side Weirs in Circular Channel—A Lazy Machine Learning Approach. *Water* **2019**, *11*, 12406. [[CrossRef](#)]
48. Rouse, H. Discharge characteristics of the free overfall. *Civ. Eng.* **1936**, *6*, 257–260.
49. Henderson, F. *Open Channel Flow*; The Macmillan Company: New York, NY, USA, 1966; p. 522.
50. Rouse, H. *The Distribution of Hydraulic Energy in Weir Flow with Relation to Spillway Design*; Massachusetts Institute of Technology: Cambridge, MA, USA, 1932.
51. Schoder, E.T.B. Precise weir measurements. *Trans. Am. Soc. Civ. Eng.* **1929**, *93*, 93. [[CrossRef](#)]

52. Eisner, F. Overfall tests to various model scales Translation, No. 42-9, U. S. Army Corps of Engineers, Waterways Experimental Station: Vicksburg, MS, USA, 1933.
53. Ghetti, A. *Effects of Surface Tension on the Shape of Liquid Jets*; Advanced Study Institute: Padova, Italy, 1966; pp. 424–475.
54. Vischer, D.; Hager, W. *Dam Hydraulics*; Wiley Series: Hoboken, NJ, USA, 1998.
55. Hager, W.H.; Schleiss, A.J.; Boes, R.M.; Pfister, M. *Hydraulic Engineering of Dams*; CRC Press: Boca Raton, FL, USA, 2021.
56. Carrillo, J.; Ortega, P.; Castillo, L.; Garcia, J. Experimental Characterization of Air Entrainment in Rectangular Free Falling Jets. *Water* **2020**, *12*, 1773. [[CrossRef](#)]
57. Raña, P.; Aneiros, G.; Vilar, J.M. Detection of outliers in functional time series. *Environmetrics* **2015**, *26*, 178–191. [[CrossRef](#)]
58. Chapra, S.; Canale, R. *Numerical Methods for Engineers*, 6th ed.; CRC Press: Boca Raton, FL, USA, 2010; p. 875.
59. Draper, N.; Smith, H. *Applied Regression Analysis*, 1st ed.; John Wiley & Sons: Hoboken, NJ, USA, 1998.
60. Montes, S. *Hydraulics of Open Channel Flow*; ASCE Press: Reston, VA, USA, 1998.

Disclaimer/Publisher’s Note: The statements, opinions and data contained in all publications are solely those of the individual author(s) and contributor(s) and not of MDPI and/or the editor(s). MDPI and/or the editor(s) disclaim responsibility for any injury to people or property resulting from any ideas, methods, instructions or products referred to in the content.